
DEEP KOOPMAN REPRESENTATION OF NONLINEAR TIME VARYING SYSTEMS

Wenjian Hao

School of Aeronautics and Astronautics Engineering
Purdue University, IN, USA
hao93@purdue.edu

Bowen Huang

Pacific Northwest National Laboratory
Richland, USA
bowen.h@pnnl.gov

Wei Pan

Department of Computer Science
University of Manchester, UK
wei.pan@tudelft.nl

Di Wu

Pacific Northwest National Laboratory
Richland, USA
di.wu@pnnl.gov

Shaoshuai Mou

School of Aeronautics and Astronautics Engineering
Purdue University, IN, USA
mous@purdue.edu

October 13, 2022

ABSTRACT

A data-driven method is developed to approximate a nonlinear time-varying system (NTVS) by a linear time-varying system (LTVS), based on Koopman Operator and deep neural networks. Analysis on the approximation error in system states of the proposed method is investigated. It is further shown by simulation on a simple NTVS that the resulted LTVS approximate the NTVS very well with small approximation errors in states. Furthermore, simulations on a cartpole further show that optimal controller developed based on the achieved LTVS works very well to control the original NTVS.

Keywords Koopman Operator; Nonlinear Time-Varying Systems; Optimal Control

1 Introduction

Data-driven control has received increasing attention since the dynamics of various autonomous systems in practice, such as underwater and bipedal robots [1], are becoming increasingly complex and sometimes unknown. Data-driven methods, such as the Koopman Operator, can address the nonlinearity of dynamics by providing a linear representation based on the data of state-control pairs [2–4]. Along this direction, two popular methods Dynamic Mode Decomposition (*DMD*) and Extending Dynamic Mode Decomposition (*EDMD*) have been widely applied in the field of fluid dynamics [5] because the resulted linear representation allows development of the optimal linear controller for nonlinear dynamics. The key idea of both *DMD* and *EDMD* is lifting the state space to a higher-dimensional space, of which the evolution is approximately linear [6]. It is still an open question how to choose nice observable functions for the lifting transformation and besides that, the potentially large lifted dimension will deteriorate the performance of real time applications.

In order to address this, some recent work [7–14] have introduced deep neural networks (DNN) into *EDMD* to approximate time-invariant systems, which utilize DNN as the observable function for Koopman operator. In these papers, the DNN observable function is tuned with respect to the collected data of state-control pairs by minimizing a properly defined loss function. Recently the time-varying dynamic mode decomposition method (*TVDMD*) was developed

in [15] to approximate a linear time-varying system (LTVS) that changes sufficiently slow. Nevertheless, this method is not directly applicable to approximate nonlinear systems with changing dynamics.

In this paper, we aim to develop a deep Koopman learning method for nonlinear time-varying systems (NTVS), i.e., achieve a LTVS to approximate the NTVS and for the development of optimal controllers. The key idea of the proposed method comes from introducing the DNN as the observable function of the Koopman Operator and adjusting the DNN and the approximated dynamical system simultaneously which is achieved by tuning the parameters of the DNN based on the latest state-control data pairs to track the unknown NTVS.

The proposed method improves the capability of approximating a NTVS compared with existing results in [7–14], with contributions summarized as follows:

- First, we propose a controllable Deep Koopman representation formulation for the NTVS and provide a practical online algorithm for the implementation purpose.
- Second, we investigate the error bound of the dynamical system states estimation introduced by the proposed method.
- Lastly, we further explore the convergence condition of the error bound with respect to the DNN observable function.

This paper is structured as follows. In Section 2, we state the problem. Section 3 presents the main results of the proposed method. The implementation results is exhibited in Section 4. Section 5 concludes the paper.

1.1 Notation

For notation simplicity, in the present work, $\|\cdot\|_2$ denotes the L_2 norm; $\|\cdot\|_F$ denotes the matrix frobenius norm; $(\cdot)^T$ denotes the matrix transpose; $\text{Trace}(\cdot)$ denotes the matrix trace; $(\cdot)^\dagger$ denotes the pseudo inverse; for a positive integer n , let \mathbf{I}_n denote the $n \times n$ identity matrix and $\mathbf{0}_n \in \mathbb{R}^n$ denote a vector with all value 0; $\lceil \cdot \rceil$ denoting the ceiling function; $\text{sgn}(\cdot)$ denotes the sign function.

2 Problem Formulation

Consider a nonlinear time-varying system (NTVS), the dynamics of which is unknown. Let $x_t \in \mathbb{R}^n$ and $u_t \in \mathbb{R}^m$ denote its state and control input at time t , respectively. Here, we assume the unknown NTVS is bounded, i.e., $|x_t| < \infty$, $|u_t| < \infty$ and $t \in \mathcal{T}$ with

$$\mathcal{T} = \begin{cases} [0, \infty), & \text{if the NTVS is in continuous-time,} \\ \{0, 1, 2, \dots\}. & \text{if the NTVS is in discrete-time.} \end{cases}$$

Suppose one only observes the unknown NTVS' states and control inputs at certain sampling time instances, i.e., the following series of data batches

$$\mathcal{B}_\tau = \{x_t, u_t : t \in t_{\mathbb{K}_\tau}\}, \quad \tau = 0, 1, 2, \dots \quad (1)$$

Here,

$$t_{\mathbb{K}_\tau} = \{t_{k_\tau}, t_{k_\tau+1}, t_{k_\tau+2}, \dots, t_{k_\tau+\beta_\tau}\} \subset \mathcal{T}$$

denotes the ordered set of sampling time instances for the τ th data batch \mathcal{B}_τ , where

$$\mathbb{K}_\tau = \{k_\tau, k_\tau + 1, k_\tau + 2, \dots, k_\tau + \beta_\tau\}, \quad \tau = 0, 1, 2, \dots$$

with β_τ positive integers such that

$$k_{\tau+1} = k_\tau + \beta_\tau, \quad \tau = 0, 1, 2, \dots$$

with $k_0 = 0$.

In this paper we aim to develop an iterative method to approximate the unknown NTVS by a linear time-varying discrete-time system (LTVDTS) based on data batches available, i.e., approximate the unknown NTVS by the following linear time-invariant system based on \mathcal{B}_τ ,

$$\hat{x}_{k+1} = \hat{A}_\tau \hat{x}_k + \hat{B}_\tau \hat{u}_k, \quad k \in \mathbb{K}_\tau, k < k_\tau + \beta_\tau. \quad (2)$$

One way to achieve such a linear approximation is by employing the Koopman Operator as in [7–14]. Namely, one achieves $\hat{A}_\tau, \hat{B}_\tau$ for (2) by finding a nonlinear mapping $g(\cdot, \theta_\tau) : \mathbb{R}^n \rightarrow \mathbb{R}^r$ parameterized by $\theta_\tau \in \mathbb{R}^q$ and matrices $A_\tau \in \mathbb{R}^{r \times r}$, $B_\tau \in \mathbb{R}^{r \times m}$, $C_\tau \in \mathbb{R}^{n \times r}$ based on the data batch \mathcal{B}_τ such that for $k \in \mathbb{K}_\tau, k < k_\tau + \beta_\tau$,

$$g(x_{k+1}, \theta_\tau) = A_\tau g(x_k, \theta_\tau) + B_\tau u_k, \quad (3)$$

$$x_{k+1} = C_\tau g(x_{k+1}, \theta_\tau), \quad (4)$$

which results in a linear system in form of (2) with

$$\hat{A}_\tau = C_\tau A_\tau C_\tau^\dagger, \quad \hat{B}_\tau = C_\tau B_\tau. \quad (5)$$

Here, $g(\cdot, \theta_\tau)$ is usually represented by a Deep Neural Networks (DNN) with a known structure but an unknown parameter vector $\theta_\tau \in \mathbb{R}^q$ to be determined based on the available data batch \mathcal{B}_τ . In the present work, the linear system (2) with $\hat{A}_\tau, \hat{B}_\tau$ (5) satisfying (3)-(4) with $g(\cdot, \theta_\tau)$ represented by a DNN is called a *Deep Koopman Representation (DKR)*.

The **problem of interest** is to develop an online update rule to achieve a Deep Koopman Representation (DKR) denoted by $\mathcal{K}_g(A_\tau, B_\tau, C_\tau, \theta_\tau)$ to the unknown NTVS such that \hat{x}_k from this DKR in (2) is close to x_k observed from the unknown NTVS in the sense that $\forall k = 1, 2, \dots$, for $\hat{u}_k = u_k$ and any given arbitrary $\hat{x}_0 \in \mathbb{R}^n$, the estimation error $|\hat{x}_k - x_k|_2$ is small especially when $\tau \rightarrow \infty$.

Remark 1 *As shown later in simulations, optimal controllers developed based on such a DKR also work very well for the optimal control of the unknown NTVS, even when it is a continuous-time system.*

3 Main Results

In this section, we first propose an algorithm to achieve a DRK to approximate an unknown NTVS and then investigate the estimation error between the state from this DKR in (2) and the observed state of the unknown NTVS.

3.1 Key Idea

Motivated by the methods based on the deep koopman operator developed in [7–14], in order to achieve an θ_τ^* , an optimal vector to θ_τ for the DKR, one only needs to solve the following optimization problem based on the data batch \mathcal{B}_τ :

$$\theta_\tau^* = \arg \min_{\theta_\tau \in \mathbb{R}^q} \{w \mathbf{L}_1(\theta_\tau) + (1-w) \mathbf{L}_2(\theta_\tau)\}. \quad (6)$$

Here,

$$\mathbf{L}_1(\theta_\tau) = \min_{A_\tau \in \mathbb{R}^{r \times r}, B_\tau \in \mathbb{R}^{r \times m}} \mathbf{L}_{11}(A_\tau, B_\tau) + \min_{C_\tau \in \mathbb{R}^{n \times r}} \mathbf{L}_{12}(C_\tau), \quad (7)$$

where

$$\mathbf{L}_{11}(A_\tau, B_\tau) = \frac{1}{\beta_\tau} \sum_{k=k_\tau}^{k_\tau+\beta_\tau-1} |g(x_{k+1}, \theta_\tau) - (A_\tau g(x_k, \theta_\tau) + B_\tau u_k)|_2, \quad (8)$$

$$\mathbf{L}_{12}(C_\tau) = \frac{1}{\beta_\tau} \sum_{k=k_\tau}^{k_\tau+\beta_\tau-1} |x_k - C_\tau g(x_k, \theta_\tau)|_2, \quad (9)$$

come from approximation of (3) and (4), respectively; and

$$\mathbf{L}_2(\theta_\tau) = (n - \text{rank}(o(\hat{A}_\tau, \hat{B}_\tau)))^2, \quad (10)$$

where $o(\hat{A}_\tau, \hat{B}_\tau)$ denotes the controllability matrix for the linear system with $\hat{A}_\tau = C_\tau A_\tau C_\tau^\dagger, \hat{B}_\tau = C_\tau B_\tau$ and A_τ, B_τ, C_τ from minimization of \mathbf{L}_{11} and \mathbf{L}_{12} (note that here, \mathbf{L}_2 is introduced such that the resulted linear system in (2) is controllable for the purpose of developing controllers later); $0 < w \leq 1$ is a constant which combines the objective of minimization of \mathbf{L}_1 to achieve a DKR and minimization of \mathbf{L}_2 for the resulted DKR to be controllable (note here when $w = 1$, one does not care about whether the resulted DKR is controllable).

In order to solve the (7), one needs to rewrite the available data batch, and objective functions \mathbf{L}_1 and \mathbf{L}_2 in compact forms. Towards this end, one lets

$$\begin{aligned} \mathbf{X}_\tau &= [x_{k_\tau}, x_{k_\tau+1}, \dots, x_{k_\tau+\beta_\tau-1}] \in \mathbb{R}^{n \times \beta_\tau}, \\ \mathbf{Y}_\tau &= [x_{k_\tau+1}, x_{k_\tau+2}, \dots, x_{k_\tau+\beta_\tau}] \in \mathbb{R}^{n \times \beta_\tau}, \\ \mathbf{U}_\tau &= [u_{k_\tau}, u_{k_\tau+1}, \dots, u_{k_\tau+\beta_\tau-1}] \in \mathbb{R}^{m \times \beta_\tau}. \end{aligned}$$

Then $\mathbf{L}_{11}(A_\tau, B_\tau)$ in (8) and $\mathbf{L}_{12}(C_\tau)$ in (9) can be rewritten as

$$\mathbf{L}_{11}(A_\tau, B_\tau) = \frac{1}{\beta_\tau} |\hat{g}(\mathbf{Y}_\tau, \theta_\tau) - (A_\tau \hat{g}(\mathbf{X}_\tau, \theta_\tau) + B_\tau \mathbf{U}_\tau)|_F, \quad (11)$$

and

$$\mathbf{L}_{12}(C_\tau) = \frac{1}{\beta_\tau} \|\mathbf{X}_\tau - C_\tau \hat{g}(\mathbf{X}_\tau, \theta_\tau)\|_F, \quad (12)$$

where

$$\begin{aligned} \hat{g}(\mathbf{X}_\tau, \theta_\tau) &= [g(x_{k_\tau}, \theta_\tau), \dots, g(x_{k_\tau + \beta_\tau - 1}, \theta_\tau)] \in \mathbb{R}^{r \times \beta_\tau}, \\ \hat{g}(\mathbf{Y}_\tau, \theta_\tau) &= [g(x_{k_\tau + 1}, \theta_\tau), \dots, g(x_{k_\tau + \beta_\tau}, \theta_\tau)] \in \mathbb{R}^{r \times \beta_\tau}. \end{aligned} \quad (13)$$

For simplicity, let $\hat{g}_{\theta_\tau}^x := \hat{g}(\mathbf{X}_\tau, \theta_\tau)$, $\hat{g}_{\theta_\tau}^y := \hat{g}(\mathbf{Y}_\tau, \theta_\tau)$. By minimization of $\mathbf{L}_{11}(A_\tau, B_\tau)$ with respect to A_τ, B_τ in (11) and minimization of $\mathbf{L}_{12}(C_\tau)$ in (12), A_τ, B_τ, C_τ can be determined by θ_τ as follows:

$$[A_\tau(\theta_\tau), B_\tau(\theta_\tau)] = \hat{g}_{\theta_\tau}^y \begin{bmatrix} \hat{g}_{\theta_\tau}^x \\ \mathbf{U}_\tau \end{bmatrix}^\dagger, \quad (14)$$

$$C_\tau(\theta_\tau) = \mathbf{X}_\tau (\hat{g}_{\theta_\tau}^x)^\dagger. \quad (15)$$

From this and (7), one has

$$\mathbf{L}_1(\theta_\tau) = \frac{1}{\beta_\tau} \sum_{k=k_\tau}^{k_\tau + \beta_\tau - 1} \left\| \begin{bmatrix} g(x_{k+1}, \theta_\tau) \\ x_k \end{bmatrix} - K_\tau(\theta_\tau) \cdot \begin{bmatrix} g(x_k, \theta_\tau) \\ u_k \end{bmatrix} \right\|_2, \quad (16)$$

with

$$K_\tau(\theta_\tau) = \begin{bmatrix} A_\tau(\theta_\tau) & B_\tau(\theta_\tau) \\ C_\tau(\theta_\tau) & 0 \end{bmatrix}.$$

Similarly, by substituting A_τ, B_τ, C_τ in (14) and (15) into (10), one has

$$\mathbf{L}_2(\theta_\tau) = (n - \text{rank}(o(\hat{A}_\tau(\theta_\tau), \hat{B}_\tau(\theta_\tau))))^2, \quad (17)$$

where

$$\hat{A}_\tau(\theta_\tau) = C_\tau(\theta_\tau) A_\tau(\theta_\tau) C_\tau(\theta_\tau)^\dagger, \hat{B}_\tau(\theta_\tau) = C_\tau(\theta_\tau) B_\tau(\theta_\tau),$$

with A_τ, B_τ, C_τ given in (14)-(15).

Remark 2 $\mathbf{L}_1(\theta_\tau)$ in (16) is a compact form of (8)-(9).

By the existing deep koopman operator method to achieve DKR by solving (6) based on each \mathcal{B}_τ , 1) one needs to compute the pseudo inverse of (14) and (15) repeatedly while solving the (6), which is memory expensive as τ increases; 2) the θ_τ is required to be initialized for each \mathcal{B}_τ , which is critical to the real time computation performance. To overcome these two limitations such that one can apply the deep koopman operator method to approximate the unknown NTVS in practice, we propose the following method.

3.2 Algorithm

Before we state the method, we make the following assumption.

Assumption 1 The matrix $\hat{g}_{\theta_\tau}^x \in \mathbb{R}^{r \times \beta_\tau}$ in (13) and $\begin{bmatrix} \hat{g}_{\theta_\tau}^x \\ \mathbf{U}_\tau \end{bmatrix} \in \mathbb{R}^{(r+m) \times \beta_\tau}$ are with full row ranks.

Remark 3 Assumption 1 is to ensure the matrices $\hat{g}_{\theta_\tau}^x \in \mathbb{R}^{r \times \beta_\tau}$ and $\begin{bmatrix} \hat{g}_{\theta_\tau}^x \\ \mathbf{U}_\tau \end{bmatrix} \in \mathbb{R}^{(r+m) \times \beta_\tau}$ are invertible. Note that Assumption 1 naturally requires $\beta_\tau \geq r + m$ and one needs to manually choose the positive integer β_τ such that it holds in practice.

Lemma 1 With the Assumption 1 hold and given the $g(\cdot, \theta_\tau), A_\tau, B_\tau, C_\tau$ and the $\mathcal{B}_{\tau+1}$, $\forall \tau \in \mathbb{N}^+$, the matrices $A_{\tau+1}(\theta_{\tau+1}) \in \mathbb{R}^{r \times r}$, $B_{\tau+1}(\theta_{\tau+1}) \in \mathbb{R}^{r \times m}$, $C_{\tau+1}(\theta_{\tau+1}) \in \mathbb{R}^{n \times r}$ can be achieved by

$$\begin{aligned} [A_{\tau+1}(\theta_{\tau+1}), B_{\tau+1}(\theta_{\tau+1})] &= (\hat{g}_{\theta_{\tau+1}}^y - [A_\tau, B_\tau] \chi_{\tau+1}) \lambda_{\tau+1} \chi_{\tau+1}^T \\ &\quad (\chi_\tau \chi_\tau^T)^{-1} + [A_\tau, B_\tau], \end{aligned} \quad (18)$$

$$C_{\tau+1}(\theta_{\tau+1}) = (\mathbf{X}_{\tau+1} - C_\tau \hat{g}_{\theta_{\tau+1}}^x) \bar{\lambda}_{\tau+1} (\hat{g}_{\theta_{\tau+1}}^x)^T (\hat{g}_{\theta_\tau}^x (\hat{g}_{\theta_\tau}^x)^T)^{-1} + C_\tau, \quad (19)$$

where

$$\chi_\tau = \begin{bmatrix} \hat{g}_{\theta_\tau}^x \\ \mathbf{U}_\tau \end{bmatrix} \in \mathbb{R}^{(r+m) \times \beta_\tau},$$

$$\begin{aligned}\lambda_{\tau+1} &= (\mathbf{I}_{\beta_{\tau+1}} + \chi_{\tau+1}^T (\chi_{\tau} \chi_{\tau}^T)^{-1} \chi_{\tau+1})^{-1} \in \mathbb{R}^{\beta_{\tau+1} \times \beta_{\tau+1}}; \\ \bar{\lambda}_{\tau+1} &= (\mathbf{I}_{\beta_{\tau+1}} + (\hat{g}_{\theta_{\tau+1}}^x)^T (\hat{g}_{\theta_{\tau}}^x (\hat{g}_{\theta_{\tau}}^x)^T)^{-1} \hat{g}_{\theta_{\tau+1}}^x)^{-1} \in \mathbb{R}^{\beta_{\tau+1} \times \beta_{\tau+1}},\end{aligned}$$

and $\hat{g}_{\theta_{\tau+1}}^x \in \mathbb{R}^{r \times \beta_{\tau+1}}, \hat{g}_{\theta_{\tau+1}}^y \in \mathbb{R}^{r \times \beta_{\tau+1}}$ are defined in (13).

Proof of the lemma 1 is shown in A.

In order to initialize the algorithm, firstly one needs to build the DNN $g(\cdot, \theta_{\tau}) : \mathbb{R}^n \rightarrow \mathbb{R}^r$ with an arbitrary nonzero vector $\theta_{\tau} \in \mathbb{R}^q$; then one achieves the matrices $A_{\tau}(\theta_{\tau}) \in \mathbb{R}^{r \times r}, B_{\tau}(\theta_{\tau}) \in \mathbb{R}^{r \times m}, C_{\tau}(\theta_{\tau}) \in \mathbb{R}^{n \times r}$ by solving (14) and (15), respectively, based on the \mathcal{B}_{τ} .

When the data batch $\mathcal{B}_{\tau+1}$ becomes available, according to the Lemma 1 one can alleviate the computation by computing the (18)-(19) instead of solving (14)-(15) repeatedly to update the $A_{\tau}(\theta_{\tau}), B_{\tau}(\theta_{\tau}), C_{\tau}(\theta_{\tau})$.

Finally, an optimal $\theta_{\tau+1}^*$ is obtained by solving (6) based on the given θ_{τ} with $A_{\tau+1}(\theta_{\tau+1}), B_{\tau+1}(\theta_{\tau+1})$ subject to (18) and $C_{\tau+1}(\theta_{\tau+1})$ subject to (19), respectively.

The algorithm is summarized as follows:

1. Initialization: Build the $g(\cdot, \theta_{\tau}) : \mathbb{R}^n \rightarrow \mathbb{R}^r$ with $\theta_{\tau} \in \mathbb{R}^q, \theta_{\tau} \neq \mathbf{0}_q$; initialize $A_{\tau}(\theta_{\tau}), B_{\tau}(\theta_{\tau})$ and $C_{\tau}(\theta_{\tau})$ by solving (14) and (15) respectively based on the \mathcal{B}_{τ} .
2. When the data batch $\mathcal{B}_{\tau+1} = \{x_k, u_k : k \in \mathbb{K}_{\tau+1}\}$ becomes available, update $A_{\tau}(\theta_{\tau}), B_{\tau}(\theta_{\tau})$ and $C_{\tau}(\theta_{\tau})$ according to (18) and (19), respectively.
3. Solve (6) to achieve the $\theta_{\tau+1}^*$.
4. Repeat the step 2-3 as the unknown NTVS evolves.

The pseudocodes is referred to B and the proposed method is referred as Deep Koopman for the NTVS (DKTV) in the following work.

3.3 Error Bound

In this subsection, we investigate the estimation error bound given by

$$e_t = \hat{x}_t - x_t, \quad t \in t_{\mathbb{K}_{\tau}}, \tau = 0, 1, \dots \quad (20)$$

where $\hat{x}_t \in \mathbb{R}^n$ denotes estimated state from the proposed method and $x_t \in \mathbb{R}^n$ denotes an arbitrary observed state of the unknown NTVS evolved from the $\{x_{t-1} \in \mathbb{R}^n, u_{t-1} \in \mathbb{R}^m\}$ (note that here, x_t does not necessarily lie in the \mathcal{B}_{τ}^x). By rewriting the formula (3) and (4), one can represent the estimated system state \hat{x}_t based on the $\mathcal{K}_g(A_{\tau}, B_{\tau}, C_{\tau}, \theta_{\tau})$, i.e.,

$$\hat{x}_t = C_{\tau}(A_{\tau}g(x_{t-1}, \theta_{\tau}) + B_{\tau}u_{t-1}). \quad (21)$$

We first show the error e_t in (20) is bounded, for which we need to make the following assumptions. For simplicity, let $\mathcal{B}_{\tau}^x \subset \mathcal{B}_{\tau}$ denote a set consisting of all the observed states $\{x_k : k \in \mathbb{K}_{\tau}\}$ in \mathcal{B}_{τ} , similarly, let $\mathcal{B}_{\tau}^u \subset \mathcal{B}_{\tau}$ denote a set consisting of all the observed control inputs $\{u_k : k \in \mathbb{K}_{\tau}\}$ in \mathcal{B}_{τ} .

Assumption 2 The observed system states and control inputs of the unknown NTVS is bounded, i.e.,

$$\|x_t\|_2 < \infty, \|u_t\|_2 < \infty, \quad t \in t_{\mathbb{K}_{\tau}}, \tau = 0, 1, 2, \dots \quad (22)$$

Assumption 3 Let σ_i^{τ} denote the i th singular value of A_{τ} with $i = 1, 2, \dots, r$. For any $A_{\tau}, \sum_{i=1}^r \sigma_i^{\tau} < 1$.

Remark 4 Assumption 3 is to ensure the $|A_{\tau}|_F < 1$. As shown in the (14), A_{τ} is determined by the DNN $g(\cdot, \theta_{\tau})$ and to make this assumption hold in practice, we refer to the existing techniques [16] which enables to apply the singular value decomposition of neural networks without computing it.

Lemma 2 Let $x_t \in \mathbb{R}^n$ denote any arbitrary observed state evolved from the $\{x_{t-1} \in \mathbb{R}^n, u_{t-1} \in \mathbb{R}^m\}$ and $\hat{x}_t \in \mathbb{R}^n$ denotes the estimated state from (21), with the Assumptions 1–3 hold, as $\tau \rightarrow \infty$, the estimation error e_t in (20) is upper bounded by

$$\|e_t\|_2 \leq \beta_{\tau} |C_{\tau}|_F L_a + L_b + L_c. \quad (23)$$

where

$$\begin{aligned}L_a &= \max_{\bar{x}_k \in \mathcal{B}_{\tau}^x} |g(\bar{x}_{k+1}, \theta_{\tau}) - A_{\tau}g(\bar{x}_k, \theta_{\tau})|_2; \\ L_b &= \max_{\bar{u} \in \mathcal{B}_{\tau}^u} |C_{\tau}B_{\tau}(\bar{u} - u_{t-1})|_2; \\ L_c &= L_1 + L_2 + L_3\end{aligned} \quad (24)$$

with $L_1 = \max_{\bar{x} \in \mathcal{B}_\tau^x} |\bar{x} - C_\tau g(\bar{x}, \theta_\tau)|_2$, $L_2 = \min_{\bar{x} \in \mathcal{B}_\tau^x} |\bar{x} - x_{t-1}|_2$, $L_3 = |x_t - x_{t-1}|_2$.

Proof of Lemma 2 is shown in C.

Remark 5 According to the Assumption 2, one notices that L_2, L_3 is bounded. Since $\mathcal{B}_\tau^x, \mathcal{B}_\tau^u$ denotes the observed states and control inputs which is known and $A_\tau, B_\tau, C_\tau, \theta_\tau$ is the achieved DKR, one can compute the L_a, L_b, L_1 immediately after solving (6), furthermore, in the following section we will show that $L_a, L_b \rightarrow 0$ when certain condition is satisfied.

3.4 Convergence Analysis of the Error Bound

In this subsection, we further investigate the convergence condition of the error bound in (23) regarding the L_a, L_b in (24) based on the Koopman Operator theory, for which we require the DNN should have at least one hidden layer and the output of the DNN $g(\cdot, \theta_\tau)$ is normalized between 0 and 1.

Definition 1 (Koopman Operator with Control) Consider the generalization of system $x_{k+1} = f(x_k, u_k)$ with $x_k \in \mathbb{R}^n, u_k \in \mathbb{R}^m$ denoting the system state and control input, respectively; and the dynamics of augmented control system states z_k, z_{k+1} is described by

$$z_{k+1} = F(z_k) := \begin{bmatrix} f(x_k, \mathbf{u}(0)) \\ \mathcal{S}\mathbf{u} \end{bmatrix},$$

where $z_k = \begin{bmatrix} x_k \\ \mathbf{u} \end{bmatrix}$ denotes the augmented control system states; $\mathcal{S}\mathbf{u}$ denotes the left shifting of the control sequence \mathbf{u} (i.e., $(\mathcal{S}\mathbf{u})(i) = \mathbf{u}(i+1)$) and $\mathbf{u}(i)$ denotes the i th element of the control sequence \mathbf{u} . Then the Koopman Operator with control $\mathcal{K} : \mathcal{H} \rightarrow \mathcal{H}$ is defined as

$$[\mathcal{K}\phi](z_k) = \phi(F(z_k)), \quad (25)$$

for each $\phi(\cdot) \in \mathbb{R}^n \times \ell(\mathcal{U}) \rightarrow \mathbb{R}$ belonging to some space of observables \mathcal{H} .

More details about the convergence analysis of the Koopman Operator refer to [17].

Let $\bar{\psi}^h$ denote the last (h th) hidden layer of $g(\cdot, \theta_\tau)$ with n_h nodes, similarly, $\bar{\psi}^o$ denotes the output layer of $g(\cdot, \theta_\tau)$ with r nodes. Before we state the results, we make the following assumption.

Assumption 4 Given a Hilbert space \mathcal{F} , the Koopman Operator $\mathcal{K} : \mathcal{F} \rightarrow \mathcal{F}$ is bounded, i.e.,

$$|\mathcal{K}|_{\mathcal{F}} = \sup_{f \in \mathcal{F}, \|f\|_{\mathcal{F}}=1} |\mathcal{K}f|_{\mathcal{F}} < \infty.$$

Definition 2 (L_2 -projection [17]) Given positive measure ν on \mathcal{M} , let $L_2(\nu)$ be the Hilbert space of all measurable functions ϕ , and \mathcal{F}_r is closed subspace of $L_2(\nu)$, where r is the size of an orthonormal basis of \mathcal{F} . We define the $L_2(\nu)$ projection of a function $\phi \in L_2(\nu)$ onto \mathcal{F}_r as

$$\begin{aligned} P_r^\nu \phi &= \arg \min_{f \in \mathcal{F}_r} \|f - \phi\|_{L_2(\nu)} = \arg \min_{f \in \mathcal{F}_r} \int_{\mathcal{M}} |f - \phi|_2^2 d\nu \\ &= \arg \min_{c \in \mathbb{R}^r} |c^\top \varphi^h - \phi|_2 d\nu, \end{aligned} \quad (26)$$

where P_r^ν is a linear projection operator.

Lemma 3 With the Assumption 4 hold, and let \mathcal{F}_{n_h} defined by $\bar{\psi}^h = [\bar{\psi}_1^h, \bar{\psi}_2^h, \dots, \bar{\psi}_{n_h}^h]^\top \in \mathbb{R}^{n_h}$ and selected from a given orthonormal basis of \mathcal{F} , i.e., $(\bar{\psi}_i^h)_{i=1}^\infty$ is an orthonormal basis of \mathcal{F} . If $\bar{\psi}^h \in \mathbb{R}^{n_h}$ forms an orthonormal basis of $\mathcal{F} = L_2(\mu)$, then P_r^μ converge strongly to the identity operator I and $\forall r, |I - P_r^\mu|_{\mathcal{F}} \leq 1$.

The proof of Lemma 3 is referred to D.

Lemma 4 Let $\phi = \sum_{i=1}^r c_i \bar{\psi}_i^o$ with $|\phi|_2 = 1$, and with the Assumption 4 hold, the approximated sequence of operators $\mathcal{K}_D P_r^\mu = P_r^\mu \mathcal{K} P_r^\mu$ will converge strongly to \mathcal{K} as n_h goes infinity, i.e.,

$$\lim_{n_h \rightarrow \infty} \int_{\mathcal{M}} |\mathcal{K}_D P_r^\mu \phi - \mathcal{K}\phi|_2 d\mu = 0. \quad (27)$$

Proof of Lemma 4 is referred to E.

Proposition 1 *With the Assumption 4 hold, according to the Lemma 3-4, for L_a, L_b in (24) we have*

$$\lim_{n_h \rightarrow \infty} L_a = 0, \quad \lim_{n_h \rightarrow \infty} L_b = 0.$$

Proof of Proposition 1 is referred to F

Remark 6 *Lemma 4 shows the convergence condition of the existing DKO method regarding the $g(\cdot, \theta_\tau)$, i.e., $\lim_{n_h \rightarrow \infty} \mathcal{K}_D P_r^\mu \phi = \mathcal{K}\phi$; it replaces the convergence condition of the EDMD method [18] which satisfies $\lim_{r \rightarrow \infty} \mathcal{K}_{EDMD} P_r^\mu \phi = \mathcal{K}\phi$, and in the present work this conclusion is used to reduce the $\beta_\tau \geq r + m$ such that we can track the unknown NTVS based on the \mathcal{B}_τ with small batch size.*

Lemma 2 states that the proposed algorithm is able to approximate the NTVS with bounded estimation error e_t in (23) with respect to L_a, L_b and L_c . Moreover, one notices that $L_a \rightarrow 0, L_b \rightarrow 0$ as $n_h \rightarrow \infty$ according to the Proposition 1. To sum up, we have the following theorem.

Theorem 1 *With the Assumptions 1-4 hold, according to the Lemma 2 and Proposition 1, when $\tau \rightarrow \infty, n_h \rightarrow \infty$,*

$$|e_t|_2 \rightarrow L_c,$$

where $L_c = L_1 + L_2 + L_3$ with $L_1 = \max_{\bar{x} \in \mathcal{B}_\tau^x} |\bar{x} - C_\tau g(\bar{x}, \theta_\tau)|_2, L_2 = \min_{\bar{x} \in \mathcal{B}_\tau^x} |\bar{x} - x_{t-1}|_2, L_3 = |x_t - x_{t-1}|_2$.

Remark 7 *Note that here the L_1 comes from the minimization of (9) which is a well-known least square minimization problem and from our simulation it is normally a small value; in order to have $L_2 \rightarrow 0$, one can reduce the sampling interval; and to make $L_3 \rightarrow 0$, one should apply the achieve DKR to estimate the state which is close to the observed \mathcal{B}_τ^x .*

4 Numerical Simulations

In this section, we first implement the proposed algorithm for the system approximation purpose, then we demonstrate the optimal control application based on the proposed algorithm. And for the deployment convenience, for the data batch \mathcal{B}_τ in (1), we set $\beta_1 = \dots = \beta_\tau = \beta$ with $\beta \geq r + m$ denoting an arbitrary positive integer and $\tau = \lceil \frac{t-\beta_0}{\beta} \rceil \in \mathbb{N}^+$ is the batch index.

4.1 System Approximation

In this subsection, the proposed algorithm is applied to approximate a 2-D example from [15]. The DNN observable function of all the following examples consists of two hidden layers with activation function $ReLU(\cdot)$; the optimizer for the DNN training is *Adam* from [19] with *learning rate* = $1e-3$ and *weight decay rate* = $1e-4$.

Before we demonstrate the experiment results, for discussion, in this subsection, $x_k = [x_1(k), \dots, x_n(k)]^T \in \mathbb{R}^n$ denotes the true dynamical states observed from the unknown NTVS; $\tilde{x}_k = [\tilde{x}_1(k), \dots, \tilde{x}_n(k)]^T \in \mathbb{R}^n$ denotes the estimated states produced by the TVDMD method [15]; $\hat{x}_k = [\hat{x}_1(k), \dots, \hat{x}_n(k)]^T \in \mathbb{R}^n$ in (21) denotes the estimated states of the proposed method (DKTV); $\tilde{e}_k = \|\tilde{x}_k - x_k\|_2$ denotes the L_2 norm of the estimation error between the TVDMD and the true system states; e_k denotes the estimation error introduced by the proposed method as defined in (20).

4.1.1 Simple 2-D NTVS

Consider the following dynamical system:

$$\dot{x}_t = M_t \cos(x_t), \quad (28)$$

where $x_t \in \mathbb{R}^2$ and the M_t is a time-varying matrix given by

$$M_t = \begin{bmatrix} 0 & (1 + \gamma t) \\ -(1 + \gamma t) & 0 \end{bmatrix}. \quad (29)$$

where γ denotes a constant that determines how fast the dynamics changes.

For the simulation, we first build the DNN ($g(\cdot, \theta) : \mathbb{R}^2 \rightarrow \mathbb{R}^6$) and set $\beta_0 = \beta = 10$; then we generate the \mathcal{B}_τ in (1) by observing the dynamics of (28) with fixed time interval $t_{k_\tau+1} - t_{k_\tau} \equiv 0.1s$ starting at $x_0 = [1, 0]^T$.

Results Analysis: We first set $\gamma = 0.8$ to evaluate the algorithm performance for NTVS that varies slowly, and show the estimation trajectories produced by the *TVDM* and the proposed method in Fig. 1. Then in Fig. 2, we show the dynamical states estimation performance of the proposed algorithm and the *TVDM* method by exhibiting the estimation error. As shown in the Fig. 1-2, when the NTVS varies slowly, both methods are able to capture the

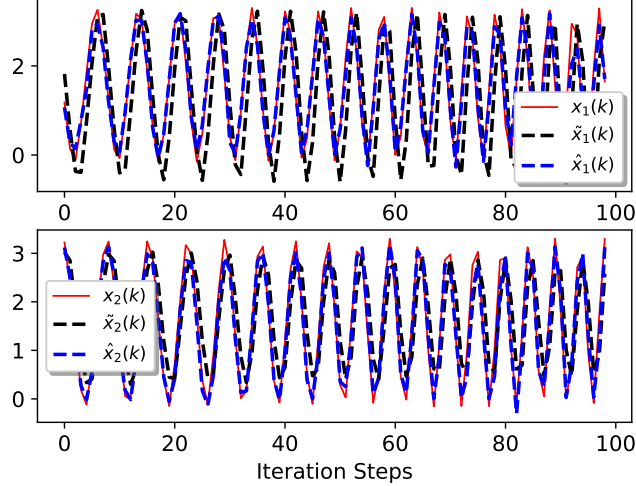


Figure 1: Estimation Trajectories of *TVDM* (Black) and *DKTV* (Blue), with $\gamma=0.8$

dynamics of NTVS, moreover, the proposed method is able to estimate the system state with smaller approximation error benefiting from its DNN observable function compared with the existing *TVDM* method.

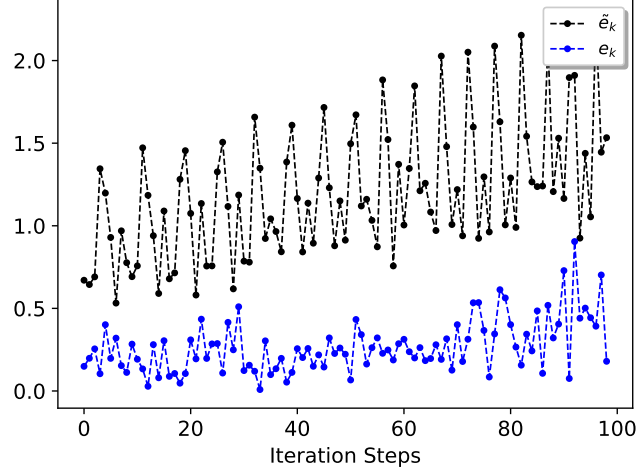


Figure 2: Dynamics States Estimation Error of *TVDM* (Black) and *DKTV* (Blue), with $\gamma=0.8$

Then we increase the changing rate of the dynamics (29) by setting $\gamma = 6$, and Fig. 3 shows that when the NTVS varies fast, the proposed method performs better compared with the existing *TVDM* method. In particular, Fig. 4 shows that the proposed method is able to approximate the dynamics varying intensively.

4.2 Optimal Control based on the Proposed Deep Koopman Learning

In this subsection, we design the optimal controller based on the proposed method for a classic Cartpole example from [20], where we make the coefficient of friction of cart on track ($\mu_c(t)$) time-varying during the simulation. And we choose the well-studied model predictive control (MPC) method to demonstrate the optimal control application

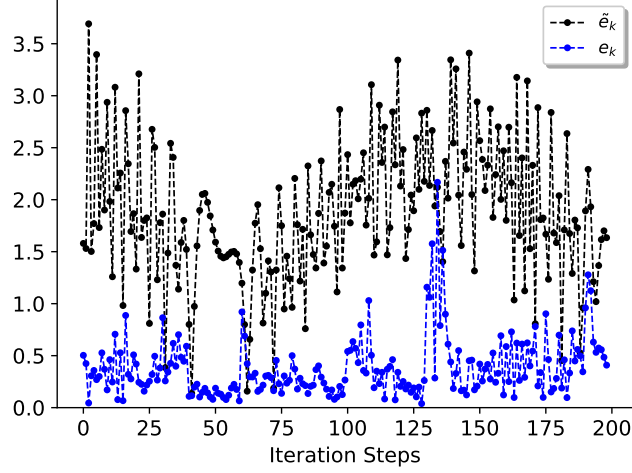


Figure 3: Dynamics States Estimation Error of *TVDMD* (Black) and *DKTV* (Blue), with $\gamma=6$

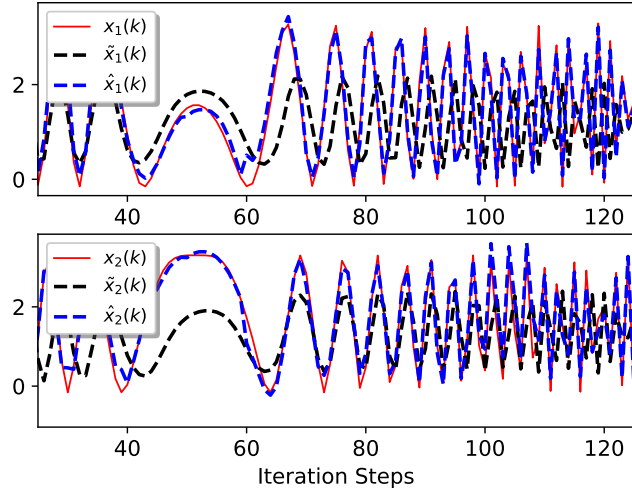


Figure 4: Estimation Trajectories of *TVDMD* (Black) and *DKTV* (Blue), with $\gamma=6$

based on the proposed algorithm, of which the optimization problem is formulated as

$$\begin{aligned}
& \min_{u_i, x_i} J(u_i, x_i) & (30) \\
& \text{subject to: } & u_i \in \mathcal{U}, x_i \in \mathcal{X}, i = k_\tau, \dots, k_\tau + l - 1 \\
& & g(x_{i+1}, \theta_\tau) = A_\tau g(x_i, \theta_\tau) + B_\tau u_i \\
& & x_i = C_\tau g(x_i, \theta_\tau) \\
& & x_{k_\tau+l} = x_l,
\end{aligned}$$

where $J(u_i, x_i)$ is defined by

$$\begin{aligned}
J(u_i, x_i) = & \sum_{i=k_\tau}^{k_\tau+l-1} (\bar{g}(x_i, \theta_\tau))^T \tilde{Q}_\tau \bar{g}(x_i, \theta_\tau) + u_i^T R u_i \\
& + g(x_l, \theta_\tau)^T \tilde{Q}_{\tau,l} g(x_l, \theta_\tau),
\end{aligned}$$

and $l \leq \beta_\tau$ is the time horizon; i is the time-index along the defined time horizon; $x_i \in \mathbb{R}^n$ and $u_i \in \mathbb{R}^m$ are the system state and control input at time step i , respectively; $\bar{g}(x_i, \theta_\tau) = g(x_i, \theta_\tau) - g(x^*, \theta_\tau)$ with x^* denoting the goal state; x_l is the terminal state; \mathcal{X} denotes the state constraint and \mathcal{U} denotes the control input constraint; $\tilde{Q}_\tau = C_\tau^T Q C_\tau \in \mathbb{R}^{r \times r}$, $Q \in \mathbb{R}^{n \times n}$, $R \in \mathbb{R}^{m \times m}$ are positive definite matrices.

4.2.1 Time-varying Cartpole Balance

In this example, the physic governing equation of the Cartpole is described as

$$\begin{aligned} \ddot{x}_t &= \frac{F_t + ml[\ddot{\theta}_t^2 \sin \bar{\theta}_t - \ddot{\theta}_t \cos \bar{\theta}_t] - \mu_t^c \text{sgn}(\dot{x}_t)}{m_c + m} \\ \ddot{\theta}_t &= \frac{g \sin \theta_t + \cos \theta_t \left[\frac{-F_t - m \ddot{\theta}_t^2 \sin \theta_t + \mu_t^c \text{sgn}(\dot{x}_t)}{m_c + m} \right] - \frac{\mu_p \dot{\theta}_t}{ml}}{l \left[\frac{4}{3} - \frac{m \cos^2 \bar{\theta}_t}{m_c + m} \right]}, \end{aligned} \quad (31)$$

where $\dot{\mu}_t^c = 0.3 \cos(t)$ with $\mu_0^c = 0.0005$ is the *time-varying* coefficient of friction of cart on track; x_t denotes the distance of the Cartpole moves from the initial position; $\bar{\theta}_t$ denotes the angle from the up position; $\dot{x}_t, \dot{\theta}_t$ denote the x-axis velocity and the angular velocity respectively; F_t denotes the continuous control input applied to the center of the mass of the cart at time step t ; $g = -9.8m/s^2$ is the gravity acceleration; $m_c = 1.0kg, m = 0.1kg$ are the mass of the cart and the pole, respectively; $l = 0.5m$ is the length of the pole; $\mu_p = 0.000002$ is the coefficient of the friction of the pole on cart.

For the simulation, we first build the DNN $(g(\cdot, \theta) : \mathbb{R}^4 \rightarrow \mathbb{R}^6)$ and set $\beta_0 = \beta = 12$; then the \mathcal{B}_τ is generated by observing the dynamics in (31) with fixed time interval $t_{k_\tau+1} - t_{k_\tau} \equiv 0.1s$. The approximated dynamics is directly applied to design the MPC controller to keep the Cartpole balanced at the up position with $\bar{\theta} = 0, \dot{\bar{\theta}} = 0$.

Results Analysis: Fig. 5 shows the trajectory of the time-varying Cartpole under the MPC control based on the proposed method. From the result, the Cartpole is able to keep the desired up position under the *DKTV*-based MPC control even though μ_k^c increases from 0.0005 to 14.288.

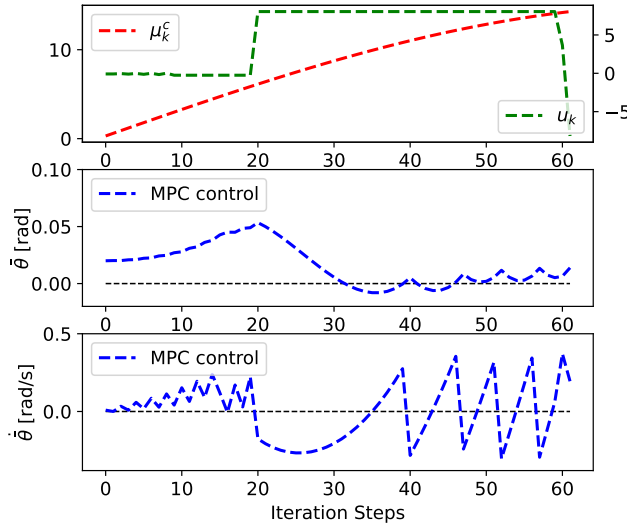


Figure 5: MPC based on the Approximated Dynamics

Remark 8 *In this subsection, we show the MPC design based on approximated linear dynamics from the proposed algorithm, when compared to the existing MPC method for the NTVS proposed in [21–23], the proposed method does not require neither the priori knowledge of the true dynamics for linearization nor the distribution information of the disturbance of the dynamical system.*

5 Conclusions

In this paper, we have provided a comprehensive online data-driven control framework and associated Deep Koopman representation for the unknown NTVS. The proposed algorithm enables the DNN observable function adaptive to track the dynamics of the unknown NTVS when the new state-control data pair is available during the controller execution. The efficiency of the proposed method is demonstrated by identifying a 2-D NTVS example when it varies slowly and fast, then the application based on the proposed method is shown in the Cartpole balancing example with time-varying

coefficient of friction of the cart on the track. In the future work, the robustness of the proposed data-driven control framework remains to be validated in the larger-scale system and the best choice of β_τ is to be investigated.

References

- [1] G. Mamakoukas, M. L. Castano, X. Tan, T. D. Murphey, Derivative-based koopman operators for real-time control of robotic systems, *IEEE Transactions on Robotics* 37 (6) (2021) 2173–2192.
- [2] I. Mezić, On applications of the spectral theory of the koopman operator in dynamical systems and control theory, in: 2015 54th IEEE Conference on Decision and Control (CDC), IEEE, 2015, pp. 7034–7041.
- [3] J. L. Proctor, S. L. Brunton, J. N. Kutz, Generalizing koopman theory to allow for inputs and control, *SIAM Journal on Applied Dynamical Systems* 17 (1) (2018) 909–930.
- [4] A. Mauroy, J. Goncalves, Linear identification of nonlinear systems: A lifting technique based on the koopman operator, in: 2016 IEEE 55th Conference on Decision and Control (CDC), IEEE, 2016, pp. 6500–6505.
- [5] I. Mezić, Analysis of fluid flows via spectral properties of the koopman operator, *Annual Review of Fluid Mechanics* 45 (2013) 357–378.
- [6] M. Korda, I. Mezić, Linear predictors for nonlinear dynamical systems: Koopman operator meets model predictive control, *Automatica* 93 (2018) 149–160.
- [7] B. Lusch, S. L. Brunton, J. N. Kutz, Data-driven discovery of koopman eigenfunctions using deep learning, *Bulletin of the American Physical Society* (2017).
- [8] E. Yeung, S. Kundu, N. Hodas, Learning deep neural network representations for koopman operators of nonlinear dynamical systems, in: 2019 American Control Conference (ACC), IEEE, 2019, pp. 4832–4839.
- [9] B. Lusch, J. N. Kutz, S. L. Brunton, Deep learning for universal linear embeddings of nonlinear dynamics, *Nature communications* 9 (1) (2018) 1–10.
- [10] Y. Li, H. He, J. Wu, D. Katabi, A. Torralba, Learning compositional koopman operators for model-based control, *arXiv preprint arXiv:1910.08264* (2019).
- [11] Y. Han, W. Hao, U. Vaidya, Deep learning of koopman representation for control, in: 2020 59th IEEE Conference on Decision and Control (CDC), IEEE, 2020, pp. 1890–1895.
- [12] D. J. Alford-Lago, C. W. Curtis, A. Ihler, O. Issan, Deep learning enhanced dynamic mode decomposition, *arXiv preprint arXiv:2108.04433* (2021).
- [13] X. Wang, Y. Kang, Y. Cao, Deep koopman operator based model predictive control for nonlinear robotics systems, in: 2021 6th IEEE International Conference on Advanced Robotics and Mechatronics (ICARM), IEEE, 2021, pp. 931–936.
- [14] P. Bevanda, M. Beier, S. Kerz, A. Lederer, S. Sosnowski, S. Hirche, Koopmanizingflows: Diffeomorphically learning stable koopman operators, *arXiv preprint arXiv:2112.04085* (2021).
- [15] H. Zhang, C. W. Rowley, E. A. Deem, L. N. Cattafesta, Online dynamic mode decomposition for time-varying systems, *SIAM Journal on Applied Dynamical Systems* 18 (3) (2019) 1586–1609.
- [16] J. Zhang, Q. Lei, I. Dhillon, Stabilizing gradients for deep neural networks via efficient svd parameterization, in: *International Conference on Machine Learning*, PMLR, 2018, pp. 5806–5814.
- [17] M. Korda, I. Mezić, On convergence of extended dynamic mode decomposition to the koopman operator, *Journal of Nonlinear Science* 28 (2) (2018) 687–710.
- [18] M. O. Williams, M. S. Hemati, S. T. Dawson, I. G. Kevrekidis, C. W. Rowley, Extending data-driven koopman analysis to actuated systems, *IFAC-PapersOnLine* 49 (18) (2016) 704–709.
- [19] D. P. Kingma, J. Ba, Adam: A method for stochastic optimization, *arXiv preprint arXiv:1412.6980* (2014).
- [20] A. G. Barto, R. S. Sutton, C. W. Anderson, Neuronlike adaptive elements that can solve difficult learning control problems, *IEEE transactions on systems, man, and cybernetics* (5) (1983) 834–846.
- [21] M. Tanaskovic, L. Fagiano, V. Gligorovski, Adaptive model predictive control for linear time varying mimo systems, *Automatica* 105 (2019) 237–245.
- [22] P. Bumroongsri, Tube-based robust mpc for linear time-varying systems with bounded disturbances, *International Journal of Control, Automation and Systems* 13 (3) (2015) 620–625.

- [23] P. Falcone, M. Tufo, F. Borrelli, J. Asgari, H. E. Tseng, A linear time varying model predictive control approach to the integrated vehicle dynamics control problem in autonomous systems, in: 2007 46th IEEE Conference on Decision and Control, IEEE, 2007, pp. 2980–2985.
- [24] G. Mamakoukas, I. Abraham, T. D. Murphey, Learning data-driven stable koopman operators, arXiv preprint arXiv:2005.04291 (2020).

A Lemma 1 Proof

Proof 1 Similar to the EDMD, we start from solving the least square problem with collected state-control pairs \mathcal{B}_τ in (1) and let $k \in \mathbb{K}_\tau$ and $x_k \in \mathbb{R}^n, u_k \in \mathbb{R}^m$ denote the observed state and control input at time step t_k respectively and

$$\begin{aligned}\mathbf{X} &= [x_{k_\tau}, x_{k_\tau+1}, \dots, x_{k_\tau+\beta_\tau-1}] \in \mathbb{R}^{n \times \beta_\tau} \\ \mathbf{Y} &= [x_{k_\tau+1}, x_{k_\tau+2}, \dots, x_{k_\tau+\beta_\tau}] \in \mathbb{R}^{n \times \beta_\tau} \\ \mathbf{U} &= [u_{k_\tau}, u_{k_\tau+1}, \dots, u_{k_\tau+\beta_\tau-1}] \in \mathbb{R}^{m \times \beta_\tau}.\end{aligned}$$

Given fixed $g(\cdot, \theta_\tau) : \mathbb{R}^n \rightarrow \mathbb{R}^r$, matrices $A_\tau \in \mathbb{R}^{r \times r}, B_\tau \in \mathbb{R}^{r \times m}$ are obtained by solving

$$\min_{A_\tau, B_\tau} |\hat{g}(\mathbf{Y}, \theta_\tau) - A_\tau \hat{g}(\mathbf{X}, \theta_\tau) - B_\tau \mathbf{U}|_F,$$

of which the unique minimum-norm solution is given by

$$[A_\tau(\theta_\tau), B_\tau(\theta_\tau)] = \hat{g}(\mathbf{Y}, \theta_\tau) \begin{bmatrix} \hat{g}(\mathbf{X}, \theta_\tau) \\ \mathbf{U} \end{bmatrix}^\dagger, \quad (32)$$

where $\hat{g}(\mathbf{X}, \theta_\tau) \in \mathbb{R}^{r \times \beta_\tau}, \hat{g}(\mathbf{Y}, \theta_\tau) \in \mathbb{R}^{r \times \beta_\tau}$ are defined by (13). Set

$$\begin{aligned}V_\tau &= \hat{g}(\mathbf{Y}, \theta_\tau) \begin{bmatrix} \hat{g}(\mathbf{X}, \theta_\tau) \\ \mathbf{U} \end{bmatrix}^T, G_\tau = \begin{bmatrix} \hat{g}(\mathbf{X}, \theta_\tau) \\ \mathbf{U} \end{bmatrix} \begin{bmatrix} \hat{g}(\mathbf{X}, \theta_\tau) \\ \mathbf{U} \end{bmatrix}^T \\ M_\tau &= [A_\tau(\theta_\tau), B_\tau(\theta_\tau)].\end{aligned}$$

Thus, Equation (32) is rewritten as

$$M_\tau = V_\tau G_\tau^{-1}.$$

As we obtain new state-control data pairs divided by

$$\begin{aligned}\Delta \mathbf{X} &= [x_{k_{\tau+1}}, x_{k_{\tau+1}+1}, \dots, x_{k_{\tau+1}+\beta_{\tau+1}-1}] \in \mathbb{R}^{n \times \beta_{\tau+1}} \\ \Delta \mathbf{Y} &= [x_{k_{\tau+1}+1}, x_{k_{\tau+1}+2}, \dots, x_{k_{\tau+1}+\beta_{\tau+1}}] \in \mathbb{R}^{n \times \beta_{\tau+1}} \\ \Delta \mathbf{U} &= [u_{k_{\tau+1}}, u_{k_{\tau+1}+1}, \dots, u_{k_{\tau+1}+\beta_{\tau+1}-1}] \in \mathbb{R}^{m \times \beta_{\tau+1}},\end{aligned}$$

then $V_{\tau+1}, G_{\tau+1}$ are updated by

$$\begin{aligned}V_{\tau+1} &= [\hat{g}(\mathbf{Y}, \theta_\tau) \hat{g}(\Delta \mathbf{Y}, \theta_{\tau+1})] \begin{bmatrix} \hat{g}(\mathbf{X}, \theta_\tau) & \hat{g}(\Delta \mathbf{X}, \theta_{\tau+1}) \\ \mathbf{U} & \Delta \mathbf{U} \end{bmatrix}^T \\ &= V_\tau + \hat{g}(\Delta \mathbf{Y}, \theta_{\tau+1}) \begin{bmatrix} \hat{g}(\Delta \mathbf{X}, \theta_{\tau+1}) \\ \Delta \mathbf{U} \end{bmatrix}^T \\ G_{\tau+1} &= \begin{bmatrix} \hat{g}(\mathbf{X}, \theta_\tau) & \hat{g}(\Delta \mathbf{X}, \theta_{\tau+1}) \\ \mathbf{U} & \Delta \mathbf{U} \end{bmatrix} \begin{bmatrix} \hat{g}(\mathbf{X}, \theta_\tau) & \hat{g}(\Delta \mathbf{X}, \theta_{\tau+1}) \\ \mathbf{U} & \Delta \mathbf{U} \end{bmatrix}^T \\ &= G_\tau + \begin{bmatrix} \hat{g}(\Delta \mathbf{X}, \theta_{\tau+1}) \\ \Delta \mathbf{U} \end{bmatrix} \begin{bmatrix} \hat{g}(\Delta \mathbf{X}, \theta_{\tau+1}) \\ \Delta \mathbf{U} \end{bmatrix}^T.\end{aligned}$$

According to the Sherman–Morrison formula:

$$(A + uv^T)^{-1} = A^{-1} - \frac{A^{-1}uv^T A^{-1}}{\mathbf{I} + v^T A^{-1}u},$$

we have:

$$\begin{aligned}M_{\tau+1} &= (V_\tau + \hat{g}(\Delta \mathbf{Y}, \theta_{\tau+1}) \chi_{\tau+1}^T) (G_\tau^{-1} - \frac{G_\tau^{-1} \chi_{\tau+1} \chi_{\tau+1}^T G_\tau^{-1}}{1 + \chi_{\tau+1}^T G_\tau^{-1} \chi_{\tau+1}}) \\ &= M_\tau - \lambda_{\tau+1} M_\tau \chi_{\tau+1} \chi_{\tau+1}^T G_\tau^{-1} \\ &\quad + \lambda_{\tau+1} \hat{g}(\Delta \mathbf{Y}, \theta_{\tau+1}) (\lambda_{\tau+1}^{-1} - \chi_{\tau+1}^T G_\tau^{-1} \chi_{\tau+1}) \chi_{\tau+1}^T G_\tau^{-1} \\ &= M_\tau - \lambda_{\tau+1} M_\tau \chi_{\tau+1} \chi_{\tau+1}^T G_\tau^{-1} \\ &\quad + \lambda_{\tau+1} \hat{g}(\Delta \mathbf{Y}, \theta_{\tau+1}) \chi_{\tau+1}^T G_\tau^{-1} \\ &= M_\tau + (\hat{g}(\Delta \mathbf{Y}, \theta_{\tau+1}) - M_\tau \chi_{\tau+1}) \lambda_{\tau+1} \chi_{\tau+1}^T G_\tau^{-1},\end{aligned}$$

where

$$\lambda_{\tau+1} = (\mathbf{I} + \chi_{\tau+1}^T G_\tau^{-1} \chi_{\tau+1})^{-1}, \chi_{\tau+1} = \begin{bmatrix} \hat{g}(\Delta \mathbf{X}, \theta_{\tau+1}) \\ \Delta \mathbf{U} \end{bmatrix},$$

and $C_{\tau+1}(\theta_{\tau+1}) \in \mathbb{R}^{n \times r}$ is proved analogically.

B Pseudocodes

Algorithm 1 Deep Koopman Representation for Time-varying Systems (DKTV)

Input: $w, \beta_0, \beta_1, \dots, \beta_\tau, \dots$
Output: $g(\cdot, \theta_\tau), A_\tau, B_\tau, C_\tau, \tau = 1, 2, \dots$
Initialization:

- Set $k = \beta_0, \tau = 0$, and empty matrices $\mathbf{X}, \mathbf{Y}, \mathbf{U}$ for the temporary data storage
- Initialize $g(\cdot, \theta_0), A_0, B_0, C_0$ based on the observed \mathcal{B}_0

while 1 do

Insert $x_k \in \mathbb{R}^n, x_{k+1} \in \mathbb{R}^n, u_k \in \mathbb{R}^m$ as new columns into $\mathbf{X}, \mathbf{Y}, \mathbf{U}$, respectively

 $k := k + 1$
if $k + 1 = \sum_{i=0}^{\tau+1} \beta_i$ **then**
Set: $\tau := \tau + 1, \mathbf{X}_\tau := \mathbf{X}, \mathbf{Y}_\tau := \mathbf{Y}, \mathbf{U}_\tau := \mathbf{U}$
Update: $A_\tau(\theta_\tau), B_\tau(\theta_\tau)$ by (18), $C_\tau(\theta_\tau)$ by (19)

Build: $\mathbf{L}(\theta_\tau)$:

$$\mathbf{L}(\theta_\tau) = w\mathbf{L}_1(\theta_\tau) + (1 - w)\mathbf{L}_2(\theta_\tau)$$

where $\mathbf{L}_1(\theta_\tau), \mathbf{L}_2(\theta_\tau)$ are defined by (16), (17), respectively

Update:

$$\theta_\tau^* = \arg \min_{\theta_\tau \in \mathbb{R}^q} \{\mathbf{L}(\theta_\tau)\}$$

$$A_\tau := A_\tau(\theta_\tau^*), B_\tau := B_\tau(\theta_\tau^*), C_\tau := C_\tau(\theta_\tau^*)$$

Reset:

$$\mathbf{X} := \mathbf{X}_\tau[:, \beta_\tau], \mathbf{Y} := \mathbf{Y}_\tau[:, \beta_\tau], \mathbf{U} := \mathbf{U}_\tau[:, \beta_\tau]$$

end

C Lemma 2 Proof

Proof 2 Suppose one has achieved the DKR $(A_\tau, B_\tau, C_\tau, \theta_\tau)$ with $\tau = 0, 1, 2, \dots$ and recall that $x_t \in \mathbb{R}^n$ and $u_t \in \mathcal{U}$ denote the system state and control input of the unknown NTVS observed at time t respectively with $t \in \mathbb{K}_\tau$; \hat{x}_t in (21) denotes the estimated state introduced by the proposed method based on the observed x_{t-1} and u_{t-1} .

Let $\bar{x}_k \in \mathcal{B}_\tau^x$ denote the closest point to the x_{t-1} in \mathcal{B}_τ^x with index $k \in \mathbb{K}_\tau$, i.e., $\bar{x}_k = \arg \min_{\bar{x} \in \mathcal{B}_\tau^x} \|x_{t-1} - \bar{x}\|_2$ and u_k denotes its corresponding control input (note that x_{t-1} is not necessarily in the \mathcal{B}_τ^x). We then extend the (20) as

$$\|e_t\|_2 = \|x_t - \hat{x}_t + \bar{x}_k - \bar{x}_k\|_2. \quad (33)$$

Here, we introduce \bar{e}_k as the local estimation error induced by the system approximation in (8) given by

$$\bar{e}_k = g(\bar{x}_k, \theta_\tau) - (A_\tau g(\bar{x}_{k-1}, \theta_\tau) + B_\tau u_{k-1}),$$

similarly, let L denote the maximum approximation error induced by the minimization of (9) by

$$L = \max_{\bar{x} \in \mathcal{B}_\tau^x} |\bar{x} - C_\tau g(\bar{x}, \theta_\tau)|,$$

which leads to

$$\begin{aligned} \|\bar{x}_k\|_2 &\leq \|C_\tau g(\bar{x}_k, \theta_\tau)\|_2 + L \\ &= \|C_\tau (A_\tau g(\bar{x}_{k-1}, \theta_\tau) + B_\tau u_{k-1}) + C_\tau \bar{e}_k\|_2 + L. \end{aligned} \quad (34)$$

By substituting the (34) and (21) into (33), we have

$$\begin{aligned} \|e_k\|_2 &\leq \|C_\tau A_\tau (g(\bar{x}_{k-1}, \theta_\tau) - g(x_{t-1}, \theta_\tau))\|_2 + \|C_\tau \bar{e}_k\|_2 \\ &\quad + \|x_t - \bar{x}_k\|_2 + \|C_\tau B_\tau (u_{t-1} - u_{k-1})\|_2 + L. \end{aligned} \quad (35)$$

For the first term of (35), we recall that the output of the DNN $(g(\cdot, \theta_\tau) : \mathbb{R}^n \rightarrow \mathbb{R}^r)$ is normalized between 0 and 1, then when $\tau \geq 1, k \geq k_1$ it is bounded by

$$\begin{aligned} \|C_\tau A_\tau^{k-k_1} \left(\prod_{j=0}^{\tau-1} A_j^{\beta_j} \right) (g(\bar{x}_0, \theta_0) - g(x_0, \theta_0))\|_2 &\leq \|C_\tau\|_F \|A_\tau^{k-k_1}\|_F \\ &\quad \left\| \prod_{j=0}^{\tau-1} A_j^{\beta_j} \right\|_F \sqrt{\tau}. \end{aligned}$$

For the second term of (35), we are inspired by the global accumulation rule of \bar{e}_k for the uncontrolled time-invariant system proposed in [24] given by

$$\mathcal{E}_k = \sum_{i=0}^{k-1} A^i \bar{e}_{k-i}. \quad (36)$$

Here, we extend (36) to the controlled time-varying system by

$$\mathcal{E}_k = \sum_{i=0}^{k-1} A_{k-i}^i \bar{e}_{k-i} + \sum_{i=0}^{k-1} A_{k-i}^i (B_{k-i-1} u_{k-i-1}). \quad (37)$$

Note that in the present work, the batch index τ is slower than the index k , hence, we need to replace the A_{k-i} , B_{k-i-1} of (37) with A_τ , B_τ and then the error bound is derived by induction, i.e., when $\tau = 1$, $k \in [k_1, k_1 + \beta_1]$,

$$\mathcal{E}_k = \sum_{l=0}^{k-k_1-1} A_1^l (\bar{e}_{k-l} + B_1 u_{k-l-1}) + A_1^{k-k_1-1} \sum_{j=1}^{\beta_0} A_0^j (\bar{e}_{k_1+1-j} + B_0 u_{k_1-j}), \quad (38)$$

when $\tau > 1$, $k \in [k_\tau, k_\tau + \beta_\tau]$,

$$\begin{aligned} \mathcal{E}_k = & \sum_{l=0}^{k-k_\tau-1} A_\tau^l (\bar{e}_{k-l} + B_\tau u_{k-l-1}) + A_\tau^{k-k_\tau-1} \left(\sum_{j=1}^{\beta_{\tau-1}} A_{\tau-1}^j \right. \\ & \left. (\bar{e}_{k_\tau+1-j} + B_{\tau-1} u_{k_\tau-j}) + \left(\sum_{i=1}^{\tau-1} \sum_{m=1}^{\beta_{i-1}} \left(\prod_{n=\tau-1}^i A_n^{\beta_n} \right) A_{i-1}^m \right) \right. \\ & \left. (\bar{e}_{k_i+1-m} + B_{i-1} u_{k_i-m}) \right), \end{aligned} \quad (39)$$

when $\tau + 1$, $k \in [k_{\tau+1}, k_{\tau+1} + \beta_{\tau+1}]$,

$$\begin{aligned} \mathcal{E}_k = & \sum_{l=0}^{k-k_{\tau+1}-1} A_{\tau+1}^l (\bar{e}_{k-l} + B_{\tau+1} u_{k-l-1}) + A_{\tau+1}^{k-k_{\tau+1}-1} \left(\sum_{j=1}^{\beta_\tau} A_\tau^j \right. \\ & \left. (\bar{e}_{k_{\tau+1}+1-j} + B_\tau u_{k_{\tau+1}-j}) + \left(\sum_{i=1}^{\tau} \sum_{m=1}^{\beta_{i-1}} \left(\prod_{n=\tau}^i A_n^{\beta_n} \right) A_{i-1}^m \right) \right. \\ & \left. (\bar{e}_{k_i+1-m} + B_{i-1} u_{k_i-m}) \right). \end{aligned} \quad (40)$$

According to (38)-(40), for $\tau > 1$, $k \in [k_2, \infty)$, the second term is bounded by

$$\begin{aligned} |C_\tau \mathcal{E}_k|_2 \leq & |C_\tau| \left(\sum_{l=0}^{k-k_\tau-1} A_\tau^l + A_\tau^{k-k_\tau-1} \left(\sum_{j=1}^{\beta_{\tau-1}} A_{\tau-1}^j + \sum_{i=1}^{\tau-1} \sum_{m=1}^{\beta_{i-1}} \right. \right. \\ & \left. \left. \left(\prod_{n=\tau-1}^i A_n^{\beta_n} \right) A_{i-1}^m \right) \right) |F L_a|. \end{aligned}$$

For the special case $\tau = 1$, $k \in [k_1, k_1 + \beta_1]$

$$|C_1 \mathcal{E}_k|_2 \leq |C_1| \left(\sum_{l=0}^{k-k_1-1} A_1^l + A_1^{k-k_1-1} \sum_{j=1}^{\beta_0} A_0^j \right) |F L_a|,$$

where

$$\begin{aligned} L_a = & \max_{\bar{x}_k \in \mathcal{B}_\tau^x, u_k \in \mathcal{U}} |\bar{e}_{k+1} + B_\tau u_k|_2 \\ = & \max_{\bar{x}_k \in \mathcal{B}_\tau^x} |g(\bar{x}_{k+1}, \theta_\tau) - A_\tau g(\bar{x}_k, \theta_\tau)|_2. \end{aligned}$$

For the last term of (35), according the Assumption 2 we have

$$|x_t - \bar{x}_k|_2 \leq \min_{\bar{x} \in \mathcal{B}_\tau^x} |x_{t-1} - \bar{x}|_2 + |x_t - x_{t-1}|_2 < \infty.$$

Let the singular value decomposition of the matrix A_τ denoted by $A_\tau = U_\tau \Sigma_\tau V_\tau^T$ with the columns of U_τ and the columns of V_τ denoting the left-singular vectors and right-singular vectors of A_τ respectively, and Σ_τ denoting a diagonal matrix consisting of the square root of the eigenvalues of $A_\tau^T A_\tau$. Then we have

$$\begin{aligned} |A_\tau|_F &= \text{Trace}(U_\tau \Sigma_\tau V_\tau^T (U_\tau \Sigma_\tau V_\tau^T)^T) = \text{Trace}(U_\tau \Sigma_\tau \Sigma_\tau^T U_\tau^T) \\ &= \text{Trace}(\Sigma_\tau \Sigma_\tau^T). \end{aligned}$$

According to the cauchy-schwarz inequality $|AB|_F \leq |A|_F |B|_F$, we have

$$\begin{aligned} \left| \prod_{j=0}^{\tau-1} A_j^{\beta_j} \right|_F &\leq |A_0^{\beta_0}|_F \cdots |A_{\tau-1}^{\beta_{\tau-1}}|_F \\ &\leq |A_0|_F \cdots |A_0|_F \cdots |A_{\tau-1}|_F \cdots |A_{\tau-1}|_F. \end{aligned} \quad (41)$$

With the Assumption 3 hold and (41), we have $\lim_{\tau \rightarrow \infty} |\prod_{j=0}^{\tau-1} (A_j^{\beta_j})|_F = 0$. Analogically, according to the triangle inequality ($|A+B|_F \leq |A|_F + |B|_F$), we have

$$\begin{aligned} \left| \sum_{l=0}^{k-k_\tau-1} A_\tau^l \right|_F &\leq |A_\tau^0|_F + \cdots + |A_\tau^{k-k_\tau-1}|_F \\ &< k - k_\tau < \beta_\tau. \end{aligned} \quad (42)$$

To sum up, let $a = |\sum_{l=0}^{k-k_\tau-1} A_\tau^l|_F$, $L_b = \max_{u \in \mathcal{B}_\tau^u} |C_\tau B_\tau (u - u_{t-1})|_2$ and $L_c = L + \min_{\bar{x} \in \mathcal{B}_\tau^x} |\bar{x} - x_{t-1}|_2 + |x_t - x_{t-1}|_2$, according to the (33)-(42) when $\tau \rightarrow \infty$, the estimation error e_t in (20) is upper bounded by

$$|e_t|_2 \leq \beta_\tau |C_\tau|_F L_a + L_b + L_c.$$

D Lemma 3 Proof

Proof 3 Let $\phi = \sum_{i=1}^r c_i \bar{\psi}_i^o$ with $|\phi|_2 = 1$, where $\bar{\psi}^o \in \mathbb{R}^r$ is the output layer of the $g(\cdot, \theta_\tau)$. Then the mapping between the output layer and the last hidden layer can be represented as

$$\bar{\psi}_i^o = \sum_{j=1}^{n_h} \theta_{i,j} \bar{\psi}_j^h, i = 1, 2, \dots, r,$$

where $\bar{\psi}_j^h$ is the j th node of $\bar{\psi}^h \in \mathbb{R}^{n_h}$; $\theta^h \in \mathbb{R}^{r \times n_h} \subset \theta_\tau$ denotes the DNN's weights of the last (h th) hidden layer; $\theta_{i,j}$ denotes the matrix entry of θ^h . Then, according to the linearity property of P_r^μ and the Parseval's identity, i.e., $\sum_{i=1}^r c_i (\sum_{j=1}^{\infty} |\theta_{i,j}|^2) = 1$, we have

$$\begin{aligned} |P_r^\mu \phi - \phi|_2 &= \left| \sum_{i=1}^r c_i \left(\sum_{j=1}^{n_h} \theta_{i,j} \bar{\psi}_j^h - \sum_{j=1}^{\infty} \theta_{i,j} \bar{\psi}_j^h \right) \right|_2 \\ &= \sum_{i=1}^r c_i \left(\sum_{j=n_h+1}^{\infty} |\theta_{i,j}|^2 \right) \xrightarrow{n_h \rightarrow \infty} 0, \end{aligned}$$

with $\sum_{i=1}^r c_i (\sum_{j=n_h+1}^{\infty} |\theta_{i,j}|^2) \leq 1$ for all r .

E Lemma 4 Proof

Proof 4 Let $\phi \in \mathcal{F}$, $\phi = P_r^\mu \phi + (I - P_r^\mu) \phi$, then by Lemma 3, we have

$$\begin{aligned} &|P_r^\mu \mathcal{K} P_r^\mu \phi - \mathcal{K} \phi|_2 \\ &= |(P_r^\mu - I) \mathcal{K} P_r^\mu \phi + \mathcal{K} (P_r^\mu - I) \phi|_2 \\ &\leq |(P_r^\mu - I) \mathcal{K} P_r^\mu \phi|_2 + |\mathcal{K} (P_r^\mu - I) \phi|_2 \\ &\leq |(P_r^\mu - I) \mathcal{K} \phi|_2 + |(P_r^\mu - I) (\mathcal{K} P_r^\mu - \mathcal{K}) \phi|_2 \\ &\quad + |\mathcal{K}|_F |(P_r^\mu - I) \phi|_2 \xrightarrow{n_h \rightarrow \infty} 0. \end{aligned} \quad (43)$$

F Proposition 1 Proof

Proof 5 Recall the L_a in (24). Since only the observed system state is lifted through the $g(\cdot, \theta_\tau)$ and let $\bar{x}_k \in \mathcal{B}_\tau^x, \bar{u}_k \in \mathcal{B}_\tau^u, \mathcal{K}_D := A_\tau, z_k := g(x_k, \theta_\tau)$. One can rewrite the L_a following the Definition 1 which leads to

$$L_a = \max_{\bar{x}_k \in \mathcal{B}_\tau^x} |\phi(F(z_k)) - [\mathcal{K}_D \phi](z_k)|_2,$$

then according to the Lemma 4, i.e., $\lim_{n_h \rightarrow \infty} \mathcal{K}_D P_\tau^\mu \phi = \mathcal{K} \phi$, we have

$$\lim_{n_h \rightarrow \infty} L_a = \max_{\bar{x}_k \in \mathcal{B}_\tau^x} |\phi(F(z_k)) - [\mathcal{K} \phi](z_k)|_2 = 0, \quad (44)$$

which leads to

$$\lim_{n_h \rightarrow \infty} |B_\tau \bar{u}_k|_2 = 0,$$

according to (3).